Marine Life Science & Technology
https://doi.org/10.1007/s42995-026-00389-y

RESEARCH PAPER

Analysis of high-fat diet tolerance in hybrid culter based on digestive enzymes, gut microbiota, and liver transcriptome

Yuxiang Wang[1] · Can Xu[1] · Xiaoyu Huang[1] · Jiaxuan Zhu[1] · Ming Wen[1] · Hongxuan Liang[1] · Yingying Yang[1] · Lang Qin[1] · Jinhui Huang[1] · Jiawang Huang[1] · Xu Huang[1,2] · Zhuangwen Mao[3] · Fangzhou Hu[1,2] · Chang Wu[1,2] · Shaojun Liu[1,2]

Received: 24 November 2025 / Accepted: 14 April 2026
© The Author(s) 2026

Abstract

Hybrid culter (Derived from lineage of *Megalobrama amblycephala* ♀ × *Culter alburnus* ♂; denoted as BTBT) is a superior cost-effective aquaculture germplasm with pronounced high-fat diet (HFD) tolerance. A 12-week feeding trial using five crude lipid gradients (3–15%) demonstrated that a dietary crude lipid content level of 9–12% was optimal for BTBT and that BTBT had significantly lower HFD mortality than its parents. We analyzed the growth performance, liver histology, digestive physiology, gut microbiota, and liver transcriptomics of BTBT individuals to elucidate the mechanism of tolerance. Growth indicators and frozen liver sections revealed that BTBT had superior growth tolerance and better liver health than its parents under HFD conditions. Notably, BTBT exhibited attenuated lipase activity, thereby mitigating HFD-induced metabolic stress. 16S rRNA sequencing revealed that under HFD conditions, BTBT maintained moderate and stable gut microbiota diversity compared with BSB, and presented significantly higher PD whole tree, Chao1 and ACE indices than TC. Liver transcriptomic profiling using the short-time-series expression miner demonstrated enhanced mitochondrial function and transcriptional regulation as dietary lipid levels increased. Weighted gene coexpression network analysis identified intermediate inheritance modules enriched for lipid/energy metabolism, antioxidant defense, immunoregulation, and tissue repair pathways (e.g., *fasn*, fatty acid-binding protein 1b, ATP synthase F1 subunit alpha, gamma-glutamyltransferase 5b, BCL2-like 1, and heat shock protein 9). Furthermore, synthesizing the parental expression patterns formed a stabilized HFD-adaptive transcriptional network. In particular, Pearson correlation analysis revealed a significant negative association between *Rhodobacter* abundance, a BTBT-enriched genus, and liver expression of the proinflammatory gene elastase 2-like, thus suggesting a causal link to reduced inflammation. Collectively, these findings demonstrate that HFD tolerance in BTBT arises from the combined effects of enhanced nutrient absorption capacity, gut microbiota stability, comprehensive regulation of multi-pathway genes, and the anti-inflammatory effects of this signature genus.

Keywords High-fat diet · Liver histology · Digestive enzyme activity · Gut microbiota · Transcriptomic regulation

Edited by Xin Yu.

Yuxiang Wang, Can Xu, and Xiaoyu Huang have contributed equally to this work.

✉ Chang Wu
wuchang@hunnu.edu.cn

✉ Shaojun Liu
lsj@hunnu.edu.cn

[1] Engineering Research Center of Polyploid Fish Reproduction and Breeding of the State Education Ministry, Hunan Normal University, Changsha 410000, China

[2] Yuelushan Laboratory, Changsha 410000, China

[3] Department of Biological and Chemical Engineering, Changsha University, Changsha 410000, China

Abbreviations

BSB	Blunt snout bream (*Megalobrama amblycephala*)
TC	Topmouth culter (*Culter alburnus*)
BTBT	The hybrid culter derived from lineage of BSB ♀ × TC ♂
HFD	High-fat diet
W_0	Initial body weight
W_t	Final body weight
W_h	Individual liver weight
W	Individual final body weight
WGR	Weight gain rate
SGR	Specific growth rate
FCR	Feed conversion ratio

Published online: 16 June 2026

HIS	Hepatosomatic index
HE	Hematoxylin-eosin
ASVs	Amplicon sequence variants
PCoA	Principal coordinates analysis
LEfSe	Linear discriminant analysis effect size
STEM	Short time-series expression miner
GO	Gene ontology
KEGG	Kyoto encyclopedia of genes and genomes
PCA	Principal component analysis
DEGs	Differentially expressed genes
GSEA	Gene set enrichment analysis
WGCNA	Weighted gene coexpression network analysis
PPI	Protein-protein interaction
GSH	Glutathione
ER	Endoplasmic reticulum
SCFA	Short-chain fatty acids
PD	Phylogenetic diversity

Introduction

With the development of intensive fish farming, the addition of high-energy-density lipids to feed can conserve protein input, reduce nitrogen pollution, and improve feed utilization (Boujard et al. 2004; Jiang et al. 2024; Thirunavukkarasar et al. 2022). Dietary lipids also provide essential nutrients, such as essential fatty acids, cholesterol, and phospholipids (Sargent et al. 1999), and the appropriate lipid levels enhance growth and feed efficiency in *Micropterus salmoides* (Guo et al. 2019). However, excessive dietary lipids disrupt the metabolic, antioxidant, and immune functions of fish, inducing inflammation and causing tissue damage (Adjoumani et al. 2017; Bonvini et al. 2015; Jin et al. 2019), which ultimately increases mortality. For instance, the winter mortality of *Salmo salar* L. is correlated with dietary lipid content (Dessen et al. 2021), and *Acanthopagrus schlegelii* is less likely to survive on a high-fat diet (HFD) than on regular diets (Zhang et al. 2025b).

With the advancement of high-throughput sequencing, 16S rRNA and liver transcriptome sequencing have emerged as primary approaches for identifying the molecular mechanisms underlying HFD-induced stress in fish (Jia et al. 2024; Ma et al. 2023). Intestinal microbiota homeostasis is essential for fish nutrient absorption and immune response (Liu et al. 2021a), and an HFD substantially alters its diversity and composition (Hooper et al. 2012; Liang et al. 2022). An HFD increases the abundance of pathogenic intestinal bacteria in *Oreochromis niloticus* while reducing that of *Bifidobacterium*, which is a producer of short-chain fatty acids (SCFAs), thereby disrupting intestinal metabolism (Ma et al. 2018). Such dysbiosis further triggers liver inflammation and lipid accumulation (Manoharan et al. 2025; Wei et al. 2024a). The liver in fish is the primary organ for lipid metabolism (Greene and Selivonchick 1987), and under HFD stress conditions, it exhibits altered lipid metabolism-related gene expression. HFD typically downregulates the β-oxidation and *pparα* genes while upregulating lipid synthesis genes, and this transcriptional imbalance promotes liver steatosis (Huang et al. 2025; Song et al. 2023). Moreover, HFD affects immune genes by upregulating liver proinflammatory factors (*TNF-α* and *IL-1β*) in *Sparus aurata* and downregulating anti-inflammatory *IL-10*, thereby impairing immunity and increasing disease susceptibility (Estensoro et al. 2016).

Numerous studies have demonstrated that specific feed supplements improve the physiological conditions of fish under HFD stress by regulating lipid or adiponectin metabolism (Xun et al. 2024). Currently, supplements with proven specific functions are primarily divided into five categories, including lipid-lowering fatty acids and drugs, vitamins and amino acids, medicinal plants and their active molecules, trace nano-minerals, and intestinal enzymes (Naiel et al. 2023). However, they are often species-specific and increase aquaculture costs. Therefore, breeding HFD-tolerant fish via germplasm improvement is an innovative solution.

Distant hybridization in fish enables breeding new varieties with heterosis, whose offspring exhibit advantages in growth, muscle nutrition, and stress resistance (Chen et al. 2023b; Luo et al. 2024; Wang et al. 2022). We previously developed a hybrid culter (BTBT) through two rounds of backcrossing from the hybrid lineage of *Megalobrama amblycephala* (blunt snout bream, BSB, ♀) × *Culter alburnus* (topmouth culter, TC, ♂) (Wu et al. 2020). BTBT exhibited a lower mortality rate than its parents under HFD (15%) conditions after 12 weeks of feeding with five crude lipid gradients (3–15%). This study analyzed the digestive enzymes, gut microbiota, and liver transcriptome of BTBT to elucidate the mechanism of HFD tolerance in BTBT and provides a reliable basis for understanding the high-fat-tolerance mechanism in hybrid fish.

Materials and methods

Sample preparation and measurement of growth indices

All three fish species (BSB, TC, and BTBT) were cultured in 45 net cages (50 fish per cage, 0.8 m × 0.8 m × 1 m) at the Polyploid Fish Breeding Engineering Center of Hunan Normal University from September to November 2023. The experiment lasted 12 weeks to obtain stable microbial and transcriptional phenotypes. All fish were examined to ensure healthy body condition, normal swimming and feeding behavior, and the absence of obvious abnormalities before commencement of the formal trial.

The cages were placed in a standard aquaculture pond with static, slightly microflow water. The water temperature was maintained at 22–28℃ (average 25℃), and the water quality parameters were monitored weekly (dissolved oxygen ≥ 5mg/L, pH 7.0–7.8, and ammonia nitrogen ≤ 0.2mg/L) to ensure optimal rearing conditions.

All three fish species were fed five experimental diets with (graded crude lipid levels of 3–15% and 40% crude protein). This range was selected, because the maternal parent BSB demonstrated marked lipid accumulation and stress at 15% dietary lipid (Lu et al. 2013). Each species was divided into five groups (1–5) with three replicates per group. The diet with a 15% crude lipid content is referred to as the HFD in this study. Diets were formulated based on four principles: nutritional balance, protein sparing, palatability, physical stability, and the practicality of raw materials. Key nutrients were kept constant, with crude lipid as the only variable. Increasing lipid levels were used to achieve protein sparing, and total energy was adjusted to support fish growth. Carboxymethyl cellulose was added as a binder to maintain pellet stability, and the cellulose content was adjusted to optimize feed hardness. High-quality, digestible ingredients, such as fishmeal, soybean meal, and peanut meal, were used for practical intensive aquaculture. Diet nutrition was verified using Qingdao STD Standard Testing Co. with near-infrared spectroscopy, and the detailed formulations are presented in Table 1.

Prior to the feeding trial, fish in each tank were collectively weighed to record the total initial body weight (W_0). Feeding was initiated at 3% of the total body weight per tank and then adjusted weekly. After 12 weeks, the fish were fasted for 24 h, followed by collective weighing of each tank to determine the total final body weight (W_t), and the survival rate for each group was calculated. The results are presented in Supplementary Fig. S1, where BTBT exhibited a significant survival advantage under HFD conditions. Subsequently, 10 fish were randomly selected from each group, euthanized, and sampled, and then, the liver, intestinal tissue, and intestinal contents were examined, as detailed in a previous study (Zhang et al. 2025c). Isolated liver tissues were rinsed with pre-cooled physiological saline, blotted dry with filter paper, and individually weighed to record the final body weight (W) and corresponding individual liver weight (W_h). The formulas for calculating the growth indices are as follows:

$$\text{Weight Gain Rate (WGR, \%)} = 100 \times \frac{Wt - W0}{W0}$$

$$\text{Specific Growth Rate (SGR, \%)} = 100 \times \frac{\ln Wt - \ln W0}{t}$$

$$\text{Feed conversion ratio} = \frac{F}{Wt - W0}$$

$$\text{Hepatosomatic Index (HSI, \%)} = 100 \times \frac{Wh}{W}$$

, where t is the duration of the feeding trial (in days), and F is the total feed intake (in g).

Table 1 Composition of the experimental diets

Item	Treatments (five diets with different lipid contents)				
	3%	6%	9%	12%	15%
Ingredients (%)					
Fishmeal[a]	40	40	40	40	40
Soybean meal	12	12	12	12	12
Peanut meal	10	10	10	10	10
Yeast	12	12	12	12	12
Fish oil	0.25	1.75	3.25	4.75	6.25
Soybean oil	0.25	1.75	3.25	4.75	6.25
Corn starch	14	10.5	7	3.5	0
Choline	6	6	6	6	6
Betaine	0.5	0.5	0.5	0.5	0.5
Vitamin and mineral premix[b]	2	2	2	2	2
Carboxymethyl cellulose	2	2	2	2	2
Dimethyl-β-propiothetin	0.05	0.05	0.05	0.05	0.05
Ethoxyquin	0.05	0.05	0.05	0.05	0.05
Cellulose	0.9	1.4	1.9	2.4	2.9
Total	100	100	100	100	100
Proximate analysis (%)					
Crude protein	37	38.1	36.8	38.2	40.3
Crude lipid	5.7	7.8	11.4	14.1	16.6
Energy values					
Gross energy (GE, MJ/kg)	18.6	19.3	20.1	20.8	21.5
Metabolizable energy (ME, MJ/kg)	13.9	14.4	15.1	15.6	16.1
Non-protein energy (NPE, MJ/kg)	9.6	10.1	11.2	11.6	11.9

[a]Fishmeal was procured from TASA, Peru, with a crude protein content of 65%

[b]Vitamin premix (mg or IU/kg): vitamin A 120,000 IU; vitamin B1, 200 mg; vitamin B2, 280 mg; vitamin B8, 240 mg; vitamin B12, 0.6 mg; VC phosphatase, 6850 mg; vitamin D3, 40,000 IU; vitamin E, 480 mg; vitamin K3, 200 mg; calcium pantothenate, 720 mg; nicotinic acid, 1000 mg; folic acid, 60 mg; biotin, 1.2 mg; and creatine, 3200 mg

Digestive enzyme activity and preparation of the frozen liver sections

After feeding BTBT and its parent lines with diets containing 3–15% crude lipid contents, the intestines of BSB, TC, and BTBT were assessed for lipase, trypsin, and cellulase activities using commercially available kits (Beijing Boxbio Science & Technology Co., Ltd.) as per the manufacturer's instructions. Each group included three biological replicates, with three technical replicates per biological replicate.

Liver samples from each group were collected for frozen sectioning. After fixation and embedding with optimal cutting temperature compound, the sections were stained with hematoxylin-eosin (HE) and Oil Red O, respectively. For HE staining, the sections were fixed, stained with HE, dehydrated, cleared, mounted with neutral balsam, and observed

under a microscope. For Oil Red O staining, the sections were stained in the dark, differentiated, counterstained with hematoxylin, mounted in glycerol-gelatin, and examined under a microscope. Morphometric analysis of liver sections stained with Oil Red O and HE was performed using ImageJ (National Institutes of Health, USA), incorporating three biological replicates per group, and the relative integrated density was calculated for quantitative analysis.

16S rRNA gene sequencing

Genomic DNA was extracted from intestinal samples, with six biological replicates per group. The DNA concentration and purity were examined by agarose gel electrophoresis. The V4–V5 regions of the 16S rRNA gene were amplified using the universal primers 515F (5'-GTGCCAGCMGCCGCGG-3') and 907R (5'-CCGTCAATTCMTTTRAGTTT-3'). Sequencing was performed on an Illumina NovaSeq 6000 platform by Shanghai OE Biotech Co., Ltd. (China), which yielded 250 bp paired-end reads. The detailed procedures were consistent with those of previous studies. Alpha and beta diversity analyses were performed using QIIME2, and alpha diversity was used to evaluate the within-sample microbial diversity. Principal coordinate analysis (PCoA) was applied to reveal differences in the gut microbiota among groups, and the linear discriminant analysis effect size (LEfSe) method was used to compare the taxonomic abundance.

Transcriptome sequencing and analysis

Total RNA was extracted from the livers of BTBT and its parental lines using TRIzol reagent, and the RNA purity and concentration were determined using a NanoDrop 2000 (Thermo Scientific, USA), with three biological replicates per group. RNA integrity was verified using an Agilent 2100 Bioanalyzer (Agilent Technologies, Santa Clara, CA, USA), and transcriptome libraries were constructed using the VAHTS Universal V5 RNA-seq Library Prep kit. Sequencing was performed by Shanghai OE Biotech Co., Ltd. (China) on an Illumina NovaSeq 6000 platform, which generated 150 bp paired-end reads. Low-quality reads were filtered to obtain clean reads, and principal component analysis (PCA) was used to assess sample similarity. Differentially expressed genes (DEGs; $P_{adj} < 0.05$, fold change (FC) > 1.5) were identified using DESeq2. Short Time-series Expression Miner (STEM) was applied to analyze gene expression patterns, followed by Gene Ontology (GO) and Kyoto Encyclopedia of Genes and Genomes (KEGG) analyses using the cluster Profiler package. Weighted gene coexpression network analysis (WGCNA) was performed using R packages (Langfelder and Horvath 2008).

Association analysis

Pearson correlation tests ($P < 0.05$) were used to identify host genes that were significantly associated with microbial abundance. Protein-protein interaction (PPI) networks were constructed using the STRING database (version 12.0) for genes. Furthermore, betweenness centrality was calculated using the Betweenness algorithm in Cytoscape (version 3.10.0) to identify potential key genes associated with herbivory.

Quantitative real-time polymerase chain reaction

Total RNA was extracted from liver tissue using TRIzol reagent, and first-strand cDNA was synthesized using a commercial reverse transcription kit (Thermo Fisher Scientific). Gene expression was analyzed by SYBR Green qPCR using the PowerUp SYBR Green Master Mix (Thermo Fisher Scientific) on a QuantStudio 5 system (Life Technologies), with *β-actin* as the internal reference. Primers were synthesized by Tsingke (Beijing, China), and their sequences are listed in Supplementary Table S3. Three biological and three technical replicates were performed for each sample. Relative gene expression levels were calculated using the $2^{-\Delta\Delta Ct}$ method.

Statistical analyses

Data analysis was performed using the Statistical Package for the Social Sciences (version 25), and graphs were generated using GraphPad Prism (version 9). Pearson correlation was used to analyze associations between the filtered and normalized transcriptome fragments per kilobase of transcript per million mapped read values and the gut microbial relative abundances. Bioinformatics analysis was conducted using the OECloud platform (https://cloud.oebiotech.com), and a two-sided $P < 0.05$ was considered statistically significant for all analyses. One-way analysis of variance followed by Bonferroni correction was applied to the growth parameters, digestive enzyme activities, and RT-qPCR data. The false discovery rate was used to control false positives in the high-throughput analyses, such as differential gene expression screening and functional enrichment analyses. All data were tested for normality and homogeneity of variance before statistical analyses.

Results

Response of the fish to the feeding regime and growth indices data

Prior to initiation of the formal trial, all fish were acclimated to the experimental pellet feed and regimen for seven days

on a 3% crude lipid basal diet, with no obvious feeding lag. During the 12-week trial, species-specific responses to dietary lipid gradients were observed. In the low-lipid groups (3–6% crude lipid), all fish demonstrated active feeding (ration completion within 30 min), bright intact body surfaces, and strong swimming vigor. However, at 9–15% lipid levels, BSB and TC exhibited reduced appetite (ration completion in 60–90 min with residuals), dull body surfaces, and diminished vigor. In contrast, BTBT maintained active feeding and normal health/appearance/vigor across all lipid gradients, including 15% HFD, thus exhibiting superior tolerance relative to its parental lines. W_0 revealed no significant differences among all dietary lipid content groups (3%–15%) and across BSB, TC, and BTBT ($P > 0.05$), except that the W_0 of TC was significantly higher in the 9% lipid group than that of BSB ($P < 0.05$). W_t, WGR, and SGR exhibited a similar trend: no significant differences across the three breeds in the 3–6% lipid groups ($P > 0.05$); at 9–15% lipid levels, these indices dropped in BSB and TC, whereas these remained high in BTBT and were significantly superior to BSB and TC at the same lipid content ($P < 0.05$). For the feed conversion ratio (FCR), no significant interbreed differences were detected in the 3–6% lipid groups ($P > 0.05$); at the 9–15% lipid levels, the FCR rose significantly with increasing lipid content ($P < 0.05$), following the order BSB > TC > BTBT ($P < 0.05$). The HSI rose gradually with the increasing dietary lipid content: there were no significant interbreed differences in the 3–9% lipid groups ($P > 0.05$); at the 12–15% lipid levels, HSI increased significantly ($P < 0.05$), with BSB significantly higher than TC and BTBT, and BTBT significantly lower than BSB and TC at the same lipid content level ($P < 0.05$).

Digestive enzyme activity and frozen liver sections

The results demonstrated that BTBT and TC consistently exhibited higher trypsin activity than BSB, with significant differences at 3% and 12% dietary crude lipid ($P < 0.05$). Furthermore, all three species revealed higher trypsin activity in medium–high- versus low-fat diets (Fig. 1A). The cellulase activity of BTBT peaked at 73.25 U/g under 6% lipid, and BTBT and BSB both demonstrated higher cellulase activity than TC (Fig. 1B). The lipase activity of BTBT was intermediate between those of the original parents, and the lipase activity reached a maximum of 47.09 U/g at 12% lipid concentration. The lipase activity of TC was consistently significantly higher than that of either or both BTBT and BSB in all groups, and the lipase activity of all three species increased with that of the dietary lipid content (Fig. 1C).

Combined HE and Oil Red O staining was used to assess liver structure and lipid deposition in BSB, TC, and BTBT under the different dietary crude lipid levels (Figs. 2 and 3). All breeds had normal livers in the 3% group. HE staining

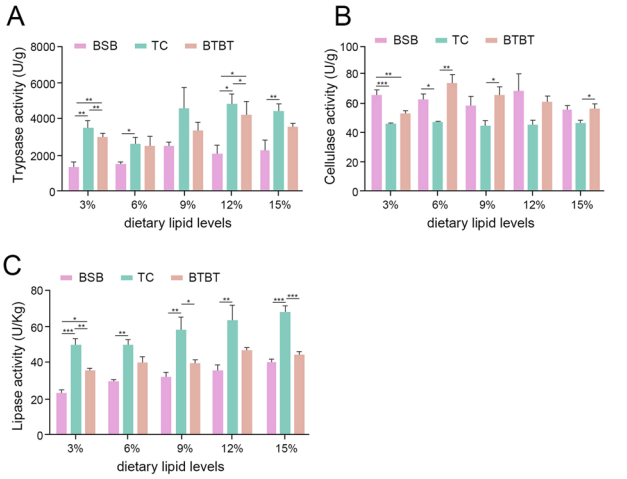

Fig. 1 Digestive enzyme activities of blunt snout bream (BSB), topmouth culter (TC), and hybrid culter derived from lineage of BSB ♀ × TC ♂ (BTBT) ($n = 3$). **A** Trypsin, **B** Cellulase, **C** Lipase. *$P < 0.05$, **$P < 0.01$, and ***$P < 0.001$

demonstrated regularly arranged hepatocytes with no obvious lipid vacuoles, and Oil Red O staining revealed a few red lipid droplets, with no intergroup differences. Liver damage and lipid deposition worsened in BSB and TC as the lipid levels increased. HE staining showed more lipid vacuoles with ≥ 6% lipid content and obvious steatosis in the 12% and 15% groups. Oil Red O staining revealed expanded red lipid droplet areas with extensive staining in the 12% and 15% groups. BTBT had significantly better liver status than BSB/TC, as HE staining identified fewer lipid vacuoles across all groups, and Oil Red O staining demonstrated much less lipid deposition. Quantitative analysis using ImageJ revealed that liver lipid vacuoles and Oil Red O-stained areas increased with dietary lipid content in BSB, TC, and BTBT. Notably, BTBT exhibited significantly lower lipid accumulation than its parental lines under medium-to-high-lipid conditions (Supplementary Fig. S2).

Gut microbial community

Intestinal contents from BSB, TC, and BTBT were collected for nucleic acid extraction, and V4–V5 regions of the 16S rRNA gene were amplified to assess bacterial diversity. A total of 6,935,982 reads (96.41% retention) were obtained after quality filtering, with 6,547 amplicon sequence variants (ASVs) identified spanning 33 phyla, 80 classes, 182 orders, 321 families, 599 genera, and 883 species (Supplementary Table S1). All samples had a Good's coverage value of 1.0, indicating comprehensive detection and accurate representation in the sequencing results. BSB demonstrated the most significant diversity index fluctuation. BSB_3 had the highest values across all seven indices among the three groups,

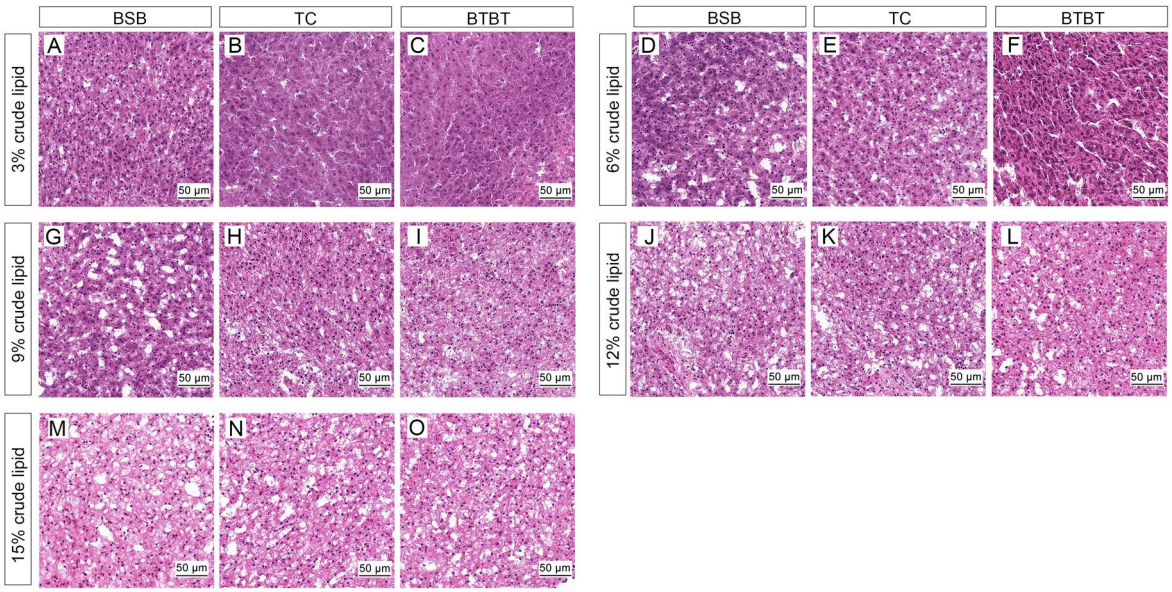

Fig. 2 Hematoxylin and eosin (HE)-stained liver sections under different dietary crude lipid levels ($n = 3$). **A–C** Sections under 3% dietary crude lipid level; **D–F, G–I, J–L, M–O** Sections under 6%, 9%, 12%, and 15% dietary crude lipid levels, respectively

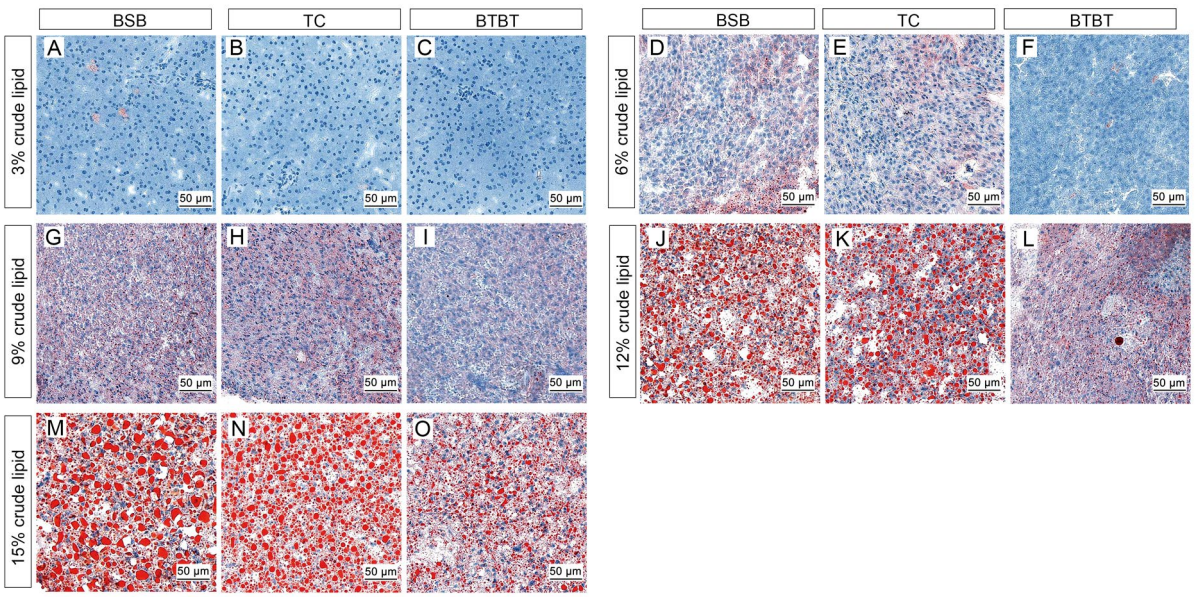

Fig. 3 Oil Red O-stained liver sections under different dietary crude lipid levels ($n = 3$). **A–C** Sections under 3% dietary crude lipid level; **D–F, G–I, J–L, M–O** sections under 6%, 9%, 12%, and 15% dietary crude lipid levels, respectively

with its phylogenetic diversity (PD) whole tree and Shannon indices significantly different from other BSB groups, indicating that the richness and diversity of gut microbiota of BSB peaked at this lipid level but decreased under low- and high-fat conditions. The α-diversity indices of TC were generally low with small fluctuations. Its PD whole tree, Chao1, and ACE indices were all lower than those of BSB and BTBT under the same dietary conditions. However, TC had higher Shannon and Simpson indices, which indicate lower gut microbiota richness but better community evenness, and both the diversity and evenness of TC_5 were both poor. The α-diversity indices of BTBT fell between those of

BSB and TC. Chao1 and observed species indices peaked at BTBT_2, and the Shannon and Simpson indices were generally high. BTBT_5 maintained moderate gut microbiota diversity without dramatic fluctuations in BSB, and its diversity indices (PD whole tree, Chao1, and ACE) were significantly higher than those of TC_5 (Table 3).

PCoA revealed that the gut microbiota composition of BTBT was more similar to that of TC across the dietary lipid levels ranging from 3 to 15% (Fig. 4A–E). At the phylum level, Proteobacteria was the dominant phylum in all three species: its relative abundance ranged from 59 to 81% in BSB, 35 to 79% in BTBT, and 32 to 56% in TC, while TC and BTBT had higher abundances of Bacteroidota and Firmicutes (Fig. 4F). At the genus level, BSB was dominated by *GKS98_freshwater_group* and *Paucibacter*, whereas TC and BTBT were mainly composed of genera such as *Acinetobacter* and *Helicobacter* (Fig. 4G). LEfSe analysis, with a linear discriminant analysis threshold set at 4, identified species-specific enriched genera: BSB had 16 characteristic genera across all groups, TC had 6 in groups 2, 3, and 5, and BTBT had 13 characteristic genera across all groups (Fig. 4H–J).

Transcriptome analysis of the response to various dietary crude lipid content levels

Reference-based transcriptome sequencing of 45 liver samples generated 304.5 Gb of CleanData, with each sample yielding 6.03–7.03 Gb of valid data, with Q30 bases accounting for 94.7–97.2% and an average GC content of 47.44% (Supplementary Table S2). Read mapping to the reference genome revealed alignment rates of 69.92–97.51% per sample. PCA indicated that BTBT samples clustered closer to TC than BSB (Supplementary Fig. S2). Using the 3% lipid group as the control, differential gene counts between groups 2–5 and group 1 were as follows: BSB (879, 1884, 296, 836); TC (225, 556, 357, 1148); BTBT (619, 252, 4330, 184) (Fig. 5A–C). STEM analysis of differential genes across the lipid levels identified 11 significant modules in

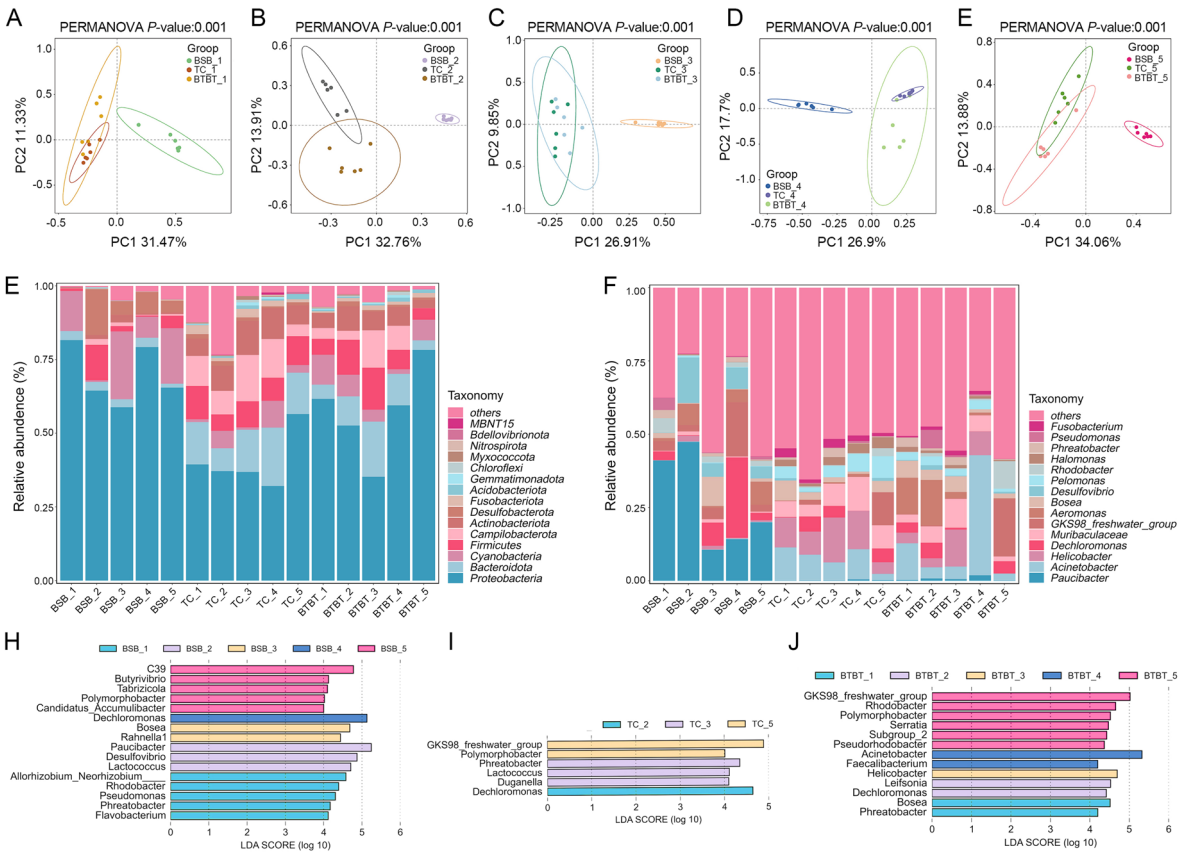

Fig. 4 Gut microbiome analysis of blunt snout bream (BSB), topmouth culter (TC), and hybrid culter derived from BSB ♀×TC ♂ (BTBT) ($n=6$). **A–E** Principal coordinate analysis (PCoA) analysis of intestinal microbiota in BSB, TC, and BTBT under 3–15% crude lipid content. **F** Histogram of the top 15 most abundant gut microbiota at the phylum level. **G** Histogram of the top 15 most abundant gut microbiota at the genus level. **H–J** Characteristic genera of BSB, TC, and BTBT under different crude lipid contents (linear discriminant analysis threshold set at 4)

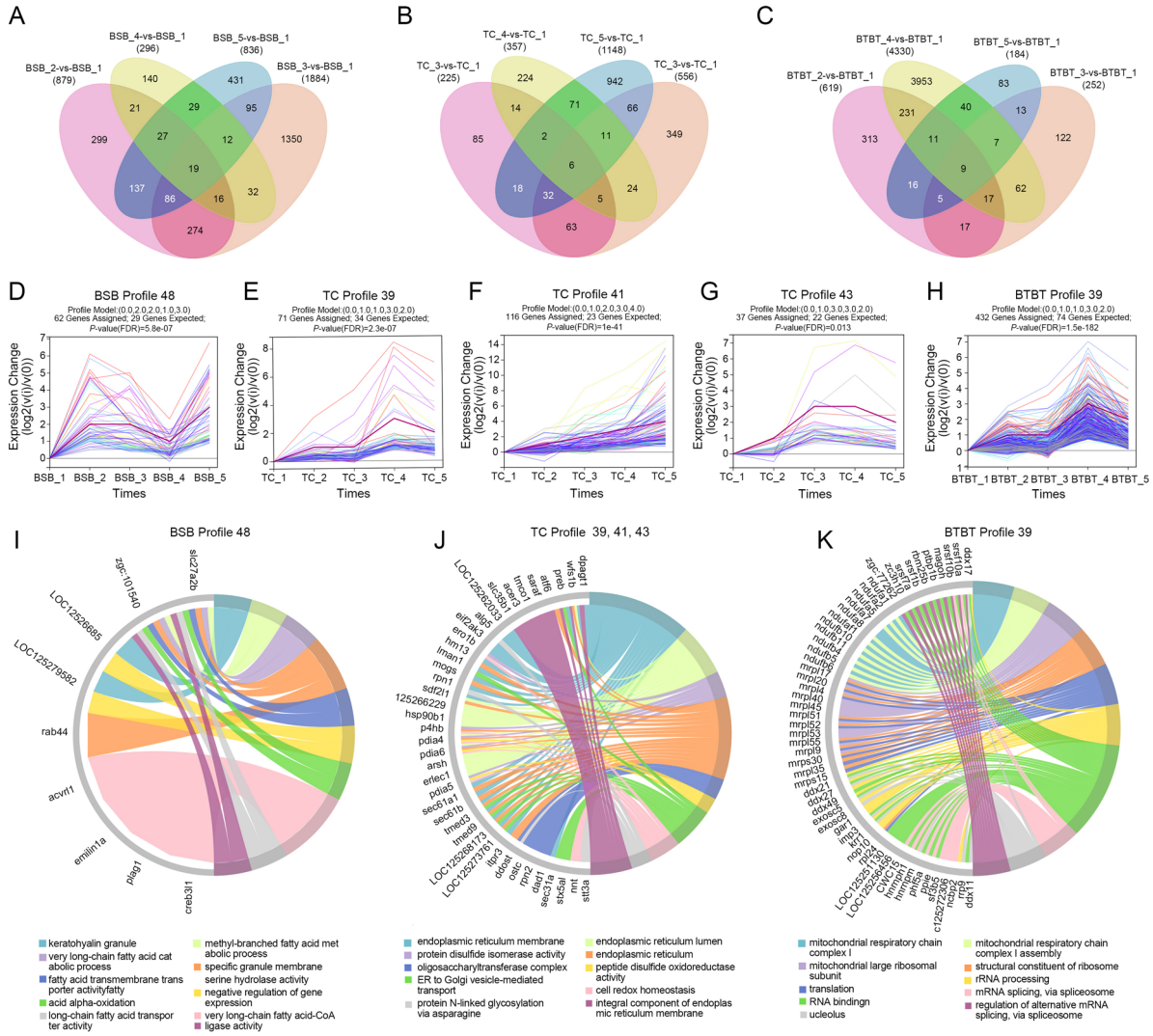

Fig. 5 Liver transcriptome analysis of blunt snout bream (BSB), topmouth culter (TC), and hybrid culter derived from lineage of BSB ♀×TC ♂ (BTBT) in response to dietary crude lipid content changes ($n=3$). **A–C** Differentially expressed genes (DEGs) within each group of BSB, TC, and BTBT. **D–H** Upward trend in BSB, TC, and BTBT. Each line represents one gene exhibiting this trend. **I–K** Gene Ontology (GO) functional enrichment TOP chord diagram of DEGs with upward trend in BSB, TC, and BTBT

BSB and 13 in TC and BTBT ($P_{adj}<0.05$, Supplementary Fig. S3). Profile 48 of BSB increased with lipid content, whereas Profile 1 decreased; Profiles 39, 41, and 43 of TC and Profile 39 of BTBT all increased with the dietary lipid content (Fig. 5D–H).

GO enrichment analysis was performed on profiles with clear upregulation or downregulation trends across the three species. Genes in Profile 48 of BSB, Profiles 39/41/43 of TC, and Profile 39 of BTBT were significantly enriched in specific pathways ($P_{adj}<0.05$). The genes in Profile 48 of BSB were enriched in lipid metabolism-centered pathways (e.g., fatty acid transport/catabolism and bile acid synthesis), protease activity regulation, cell structure formation, substance transport, and negative regulation of immune factors, which suggests the involvement lipid metabolism and immune homeostasis regulation in BSB in response to lipid dietary changes (Fig. 5I). Genes in Profiles 39, 41, and 43 of TC were enriched in endoplasmic reticulum (ER)-centered pathways (e.g., protein folding, glycosylation, transmembrane transport, and stress response) and mitochondrial inner membrane structure, which indicates the adaptation of TC via regulating ER-mediated protein processing (Fig. 5J). Genes in Profile 39 of BTBT were enriched in mitochondrial function-centered pathways (e.g., respiratory chain assembly, electron transport, and energy synthesis), RNA processing and protein synthesis (e.g., mRNA splicing,

rRNA metabolism, and translation), and nuclear structure/regulation, which suggests the adaptation of BTBT through regulating energy metabolism and genetic information processing (Fig. 5K).

Transcriptome and gut microbiota analysis under HFD conditions

Gene set enrichment analysis (GSEA) was performed on 15 KEGG lipid metabolism pathways in BSB, TC, and BTBT to further investigate the high survival rate of BTBT under HFD conditions. BTBT_5 had expression advantages in 10 pathways versus BSB_5 and 8 versus TC_5; TC_5 had 8 advantages versus BSB_5 (Fig. 6A–C). In terms of DEGs, BTBT_5 vs. BSB_5 had 1477 upregulated and 1389 downregulated genes, and BTBT_5 vs. TC_5 had 961 upregulated and 1300 downregulated genes, and BSB_5 versus TC_5 had 2748 upregulated and 3261 downregulated genes (Fig. 7A). Merged DEGs underwent WGCNA (power = 24, SD threshold = 0.5, merge threshold = 0.25, min module genes = 20, and cut height = 1), yielding nine modules. Significant modules were grey60, green, cyan, midnight blue, brown, black, and magenta. They were then divided into three categories according to the expression of the BTBT_5 genes: lowest expression, grey60; green/cyan/midnight blue/brown/black (BTBT_5 expression between parents); and highest expression, magenta (Fig. 7B, C).

GO and KEGG enrichment analyses were performed for genes in the three module types. The grey60 module (lowest expression in BTBT_5) was significantly enriched in three GO categories ($P_{adj} < 0.05$), specifically protease activity and proteolysis (serine-type endopeptidase activity and serine hydrolase activity), digestion and cell structure (digestion and keratohyalin granule), and immunity and signal regulation (positive regulation of protein kinase B signaling and lymphocyte chemotaxis), with no significant KEGG pathways detected (Fig. 7D, G). Modules with intermediate BTBT_5 expressions had GO pathways that were enriched in lipid metabolism (triglyceride catabolism and cholesterol transport regulation), energy metabolism (respiratory chain and tricarboxylic acid cycle), antioxidant activity (glutathione (GSH) transferase activity and hydrogen peroxide catabolism), immunity (complement activation and positive regulation of chemokine secretion), and tissue repair (hepatocyte differentiation). Furthermore, their KEGG pathways were enriched in lipid metabolism (PPAR signaling pathway and primary bile acid biosynthesis), energy metabolism (oxidative phosphorylation and citrate cycle), and antioxidant activity (GSH metabolism and drug metabolism-cytochrome P450) ($P_{adj} < 0.05$, Fig. 7E, H). The magenta module (highest expression in BTBT_5) indicated no significant pathways in either GO or KEGG enrichment ($P_{adj} > 0.05$; Fig. 6F, I).

Typical inflammatory factor expression was analyzed as the grey60 module genes (lowest expression in BTBT_5) were significantly enriched in immune pathways linked to inflammation, which revealed that TC_5 had significantly higher levels than BSB_5 and BTBT_5 (Fig. 8A). *Rhodobacter*, a signature microbiota of BTBT_5 (Fig. 4J), was more abundant in BTBT_5 than in its parent lines (Fig. 8B) and is known to enhance fish liver antioxidant

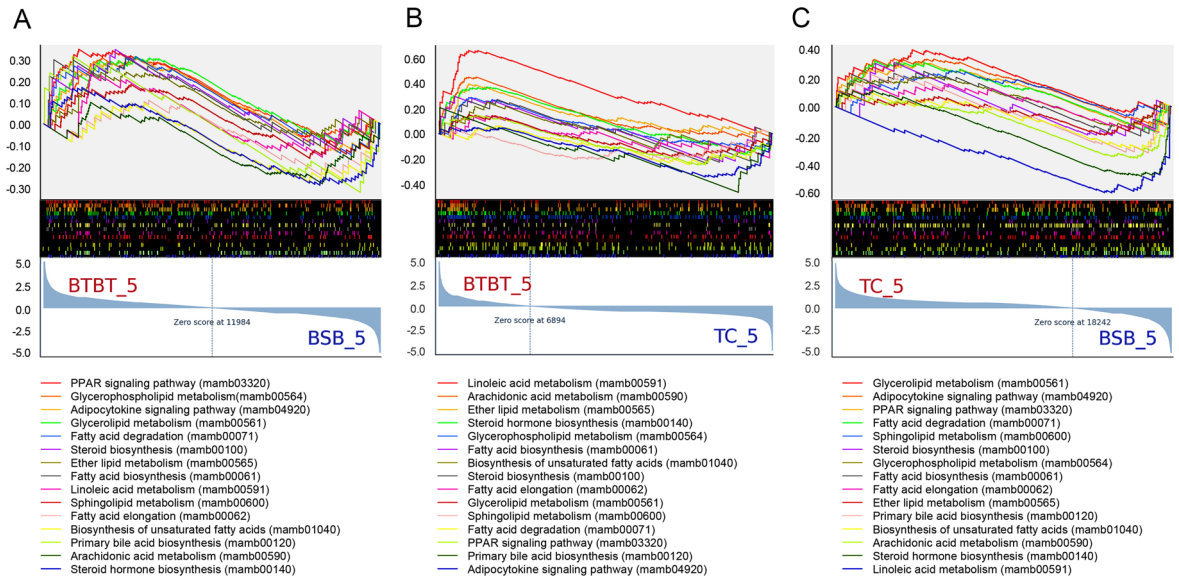

Fig. 6 GSEA analysis of lipid metabolism pathways among blunt snout bream (BSB), topmouth culter (TC), and hybrid culter derived from lineage of BSB ♀ × TC ♂ (BTBT) under high-fat diet (HFD) conditions ($n = 3$). **A** BTBT vs BSB. **B** BTBT vs TC. **C** TC vs BSB

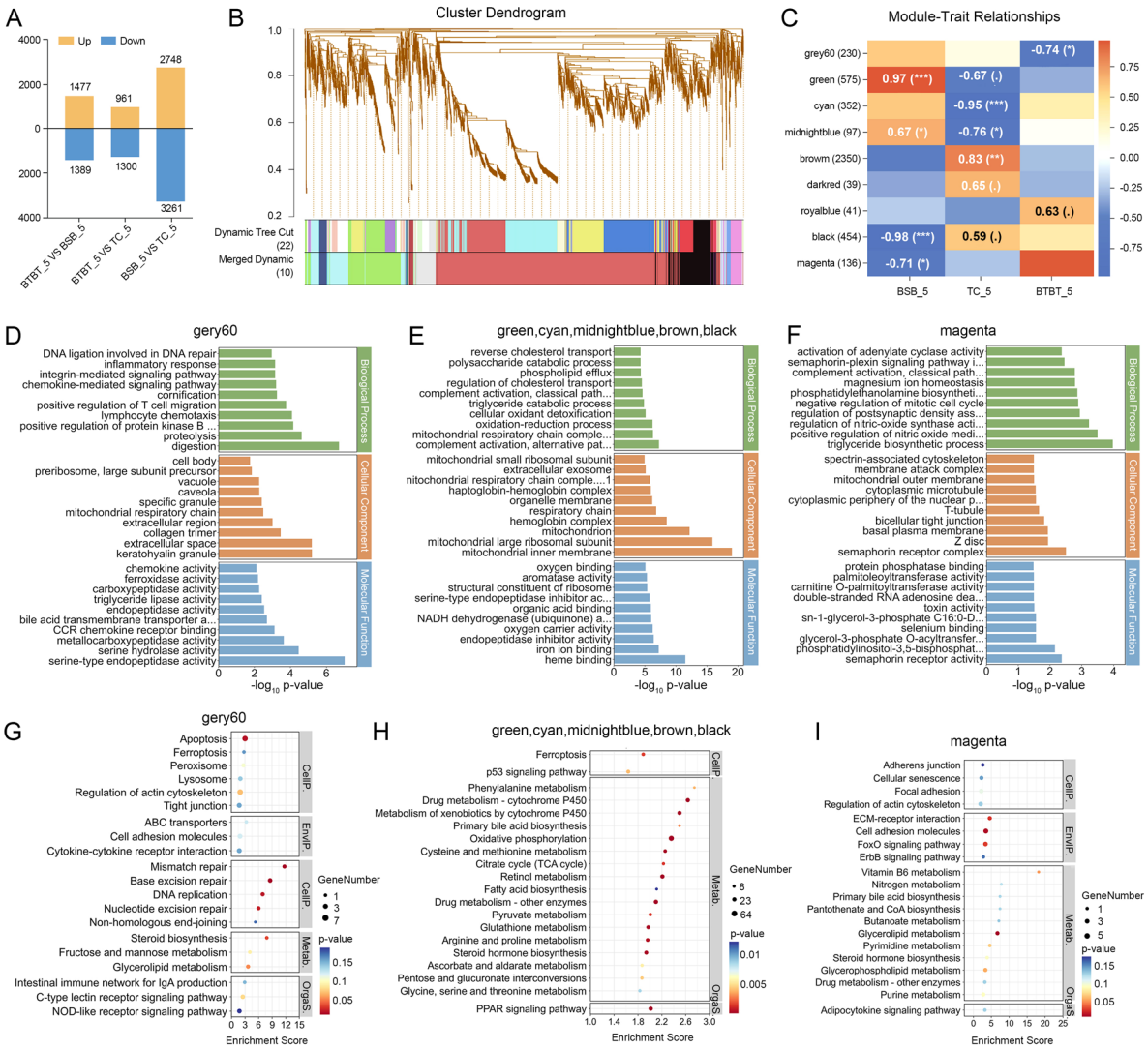

Fig. 7 Liver transcriptome analysis of blunt snout bream (BSB), topmouth culter (TC), and hybrid culter derived from lineage of BSB ♀×TC ♂ (BTBT) under high-fat diet (HFD) conditions ($n=3$). **A** DEGs among BSB, TC, and BTBT. **B–C** WGCNA analysis of DEGs among BSB, TC, and BTBT. **D–F** GO enrichment analysis of the top 30 of the three modules (BTBT with the lowest, highest, and parental intermediate expression levels) among DEGs. **G–I** KEGG enrichment analysis top 20 of the three modules (BTBT with the lowest, highest, and parental intermediate expression levels) among DEGs

function (Zhou et al. 2025). Pearson correlation analysis demonstrated that *Rhodobacter* was generally negatively correlated with grey60 module proinflammatory genes, such as lymphocyte chemotaxis, with a significant negative correlation with the elastase 2-like (*ela2l*) gene (Fig. 8C). In modules with intermediate BTBT_5 expressions, enriched pathways were divided into five categories: lipid metabolism, energy metabolism, antioxidation, immunity, and tissue repair (Supplementary Table S4). Genes in these categories were used to construct a PPI network using STRING (confidence score = 0.7), and the key HFD-responsive genes were identified using betweenness centrality (Fig. 8D–H). Key genes related to lipid metabolism included fatty acid synthase and fatty acid-binding protein 1b (*fabp1b.1*). Critical genes related to energy metabolism included ATP synthase F1 subunit alpha (*atp5fa1*), and important genes related to antioxidation included gamma-glutamyltransferase 5b (*ggt5b*), while those related to immunity included BCL2-like 1 (*bcl2l1*). In addition, key genes related to tissue repair included heat shock protein 9 (*hspa9*).

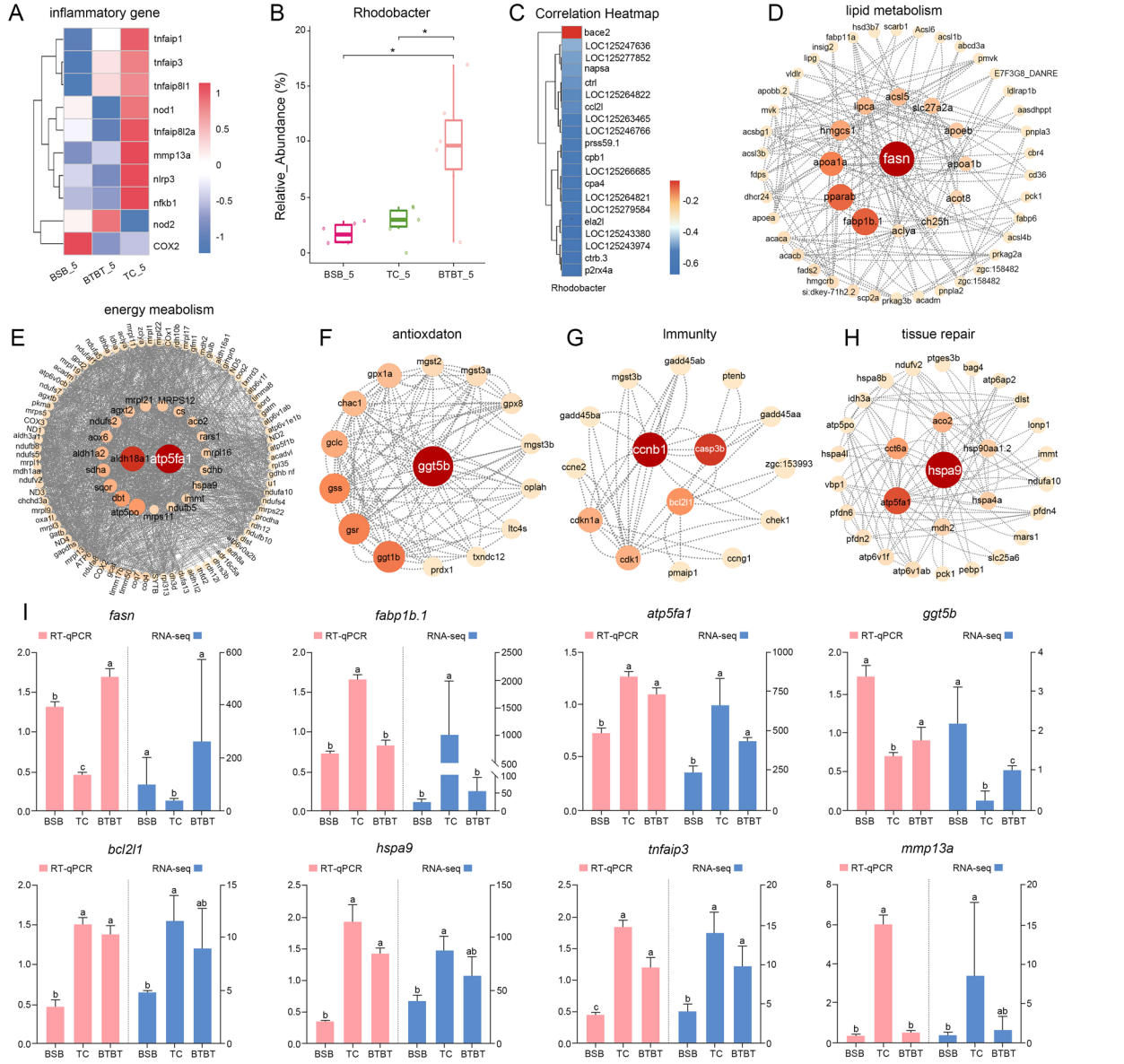

Fig. 8 Association analysis and validation of gene expression levels. **A** Expression levels of typical inflammatory genes in the livers of blunt snout bream (BSB), topmouth culter (TC), and hybrid culter derived from lineage of BSB ♀ × TC ♂ (BTBT) under high-fat diet (HFD) conditions. **B** Relative abundance of *Rhodobacter* in BSB, TC, and BTBT under HFD conditions. **C** Correlation heatmap between *Rhodobacter* abundance and proinflammatory genes in the grey60 module. $*P < 0.05$. **D–H** Protein–protein interaction (PPI) network of genes related to lipid metabolism, energy metabolism, antioxidants, immunity, and tissue repair in the module that has BTBT expression level between those of its parents among DEGs under HFD conditions. **I** Relative mRNA levels of DEGs in BSB, TC, and BTBT determined by RT-qPCR ($n = 3$). Different lowercase letters indicate significant differences ($P < 0.05$)

RT-qPCR validation

The expression levels of six key regulatory genes (*fasn*, *fabp1b.1*, *atp5fa1*, *ggt5*, *bcl2l1*, and *hspa9*) and two inflammatory genes (*mmp13a* and *tnfaip3*) under HFD conditions were assessed to validate the liver transcriptome results of the three fish species. RT-qPCR was used to quantify the expression levels of these genes, and the results were highly consistent with those from the RNA-seq analysis (Fig. 8I). This confirmed the expression characteristics of the key genes and the reliability of the RNA-seq data.

Discussion

Superior high-fat tolerance reflected by growth and liver health in BTBT

In intensive aquaculture, HFDs reduce nitrogen excretion via protein-sparing effects but can cause metabolic disorders and immunosuppression (including death) when lipid intake exceeds fish tolerance (Desouky et al. 2025; He et al. 2024). Previous mitigation strategies relied on feed additives, which raise costs; however, germplasm improvement is a more direct approach. We obtained high-fat-tolerant BTBT by hybridizing herbivorous BSB and carnivorous TC, followed by two backcrosses (Wei et al. 2024b; Wu et al. 2020; Yin et al. 2021). Fish growth indicators are intuitive quantitative metrics for assessing growth status and health (Chen et al. 2023a). In this study, the core growth indicators (W_t, WGR, and SGR) demonstrated a breed-lipid level interaction. Furthermore, there were no interbreed differences in the low-lipid groups, whereas WGR and SGR were decreased in BSB and TC under high-lipid conditions, and BTBT exhibited greater tolerance. This aligned with the general rule that lipids exert a protein-sparing effect to optimize growth, but excess lipids exceed the metabolic capacity and thus inhibit growth (Khadim et al. 2025). The high-lipid group FCR followed the pattern of BSB > TC > BTBT, which suggests the superior nutrient utilization of BTBT over its parent lines under high-lipid conditions. Significant interbreed HSI differences were observed in the high-lipid groups, with BTBT revealing the lowest (Table 2). This was consistent with the frozen liver staining results, where HE staining revealed hepatocytes arranged in a regular pattern, with a few lipid vacuoles. In addition, Oil Red O staining indicated low-lipid deposition, thereby confirming the superior liver health of BTBT (Chi et al. 2024; Sun et al. 2025) (Figs. 2 and 3). ImageJ quantitative analysis revealed that liver lipid vacuoles and Oil Red O-stained positive areas in BTBT were significantly lower than those in its parental lines under high-fat conditions, further confirming its lower liver lipid accumulation (Supplementary Fig. S2).

Digestive enzyme traits contributing to HFD adaptation in BTBT

Digestive enzyme activity reflects nutrient utilization (Jiao et al. 2023). Digestive enzyme assays revealed that the BTBT liver exhibited higher trypsin activity than the BSB and closely matched that of the paternal TC. Its cellulase activity was comparable to that of BSB and significantly exceeded that of TC. While the lipase activity of BTBT was generally intermediate between the two parent lines, it decreased significantly on an HFD and was lower than that of TC. Notably, lipase activity increased with dietary lipid levels in BSB and TC (Fig. 1A–C), which is consistent with findings in *Brachymystax lenok* and hybrid tilapia (*Oreochromis niloticus* × *O. aureus*) (Chang et al. 2018; Han et al. 2011). However, BTBT exhibited reduced lipase activity under HFD conditions compared with the 12% lipid diet. BTBT exhibited strong cellulase and trypsin activities, as well as moderate lipase activity. Under an HFD, a moderate reduction in lipase activity helps inhibit the adverse effects of high-fat content (Zhang et al. 2020). These indicate that the digestive enzyme activity characteristics of BTBT result from the synergy of genetic inheritance, which lays the core foundation, and compensatory physiological regulation as an optimized adaptation. These parent-combined enzymatic traits enable BTBT to alleviate the adverse effects of high fat, efficiently absorb proteins, and maintain intestinal utilization of plant components through cellulase under HFD conditions, thereby supporting long-term HFD adaptation (Thapa et al. 2020; Zhang and Yang 2016).

Gut microbiota stability and composition favor BTBT under high-fat stress

Intestinal microbiota homeostasis is key for host nutrient metabolism and immune defense (Jandhyala et al. 2015; Min and Rhee 2015). Moreover, 16S rRNA sequencing revealed that α-diversity of the BSB microbiota fluctuated sharply with the lipid content concentration (i.e., HFD disrupted homeostasis); for TC, it was low but had high evenness (i.e., some HFD resistance), and that of BTBT was between those of the parent lines (i.e., stable under high fat, but richer than TC) (Table 3). This stability supports the HFD adaptation of BTBT, as microbiota imbalance raises disease susceptibility under nutritional stress (Li et al. 2025). PCoA indicated that the microbiota composition of BTBT was more similar to that of TC across the lipid concentrations (Fig. 4A–E). Herbivorous BSB has a lower tolerance to high fat than carnivorous TC (Li et al. 2010; Zhang et al. 2016); accordingly, bacteria in BTBT that are similar to those in TC may aid its HFD adaptation. In composition, BTBT and TC had higher Firmicutes abundance than BSB (Fig. 4F). Firmicutes are associated with lipid degradation and SCFA synthesis, thereby optimizing lipid metabolism and maintaining the intestinal barrier integrity under HFD (Liu et al. 2021b; Sharma et al. 2025). At the genus level, BTBT and TC had highly similar gut microbiota (Fig. 4G), which were closely related to their shared digestive physiological traits; both were dominated by the lipase-producing genus *Acinetobacter* (Snellman and Colwell 2004). These dominant

Table 2 Growth indices data

Growth index	Lipid content	BSB	TC	BTBT
W_0 (g)	3.00%	5.15 ± 0.05^{a}	5.22 ± 0.10^{a}	5.17 ± 0.07^{a}
	6.00%	5.19 ± 0.07^{a}	5.27 ± 0.08^{a}	5.22 ± 0.08^{a}
	9.00%	5.14 ± 0.07^{b}	5.33 ± 0.14^{a}	5.21 ± 0.09^{ab}
	12.00%	5.17 ± 0.05^{a}	5.34 ± 0.07^{a}	5.24 ± 0.07^{a}
	15.00%	5.15 ± 0.07^{a}	5.25 ± 0.11^{a}	5.29 ± 0.17^{a}
W_t (g)	3.00%	28.37 ± 2.40^{a}	29.64 ± 2.88^{a}	30.33 ± 1.86^{a}
	6.00%	31.64 ± 2.84^{a}	33.14 ± 2.82^{a}	33.8 ± 1.53^{a}
	9.00%	30.17 ± 0.35^{b}	32.00 ± 0.50^{b}	35.62 ± 2.29^{a}
	12.00%	27.83 ± 0.35^{b}	30.17 ± 0.65^{b}	33.56 ± 1.24^{a}
	15.00%	24.55 ± 0.90^{c}	27.48 ± 1.13^{b}	31.46 ± 1.00^{a}
WGR (%)	3.00%	450.84 ± 50.72^{a}	468.71 ± 62.34^{a}	486.37 ± 28.99^{a}
	6.00%	509.9 ± 58.86^{a}	528.73 ± 50.31^{a}	548.36 ± 38.57^{a}
	9.00%	487.00 ± 13.01^{b}	500.42 ± 24.57^{b}	584.09 ± 41.63^{a}
	12.00%	438.03 ± 6.33^{b}	464.68 ± 16.85^{ab}	540.72 ± 29.25^{a}
	15.00%	376.57 ± 20.76^{b}	423.84 ± 29.98^{ab}	495.75 ± 35.86^{a}
SGR (%)	3.00%	2.03 ± 0.11^{a}	2.06 ± 0.13^{a}	2.10 ± 0.06^{a}
	6.00%	2.15 ± 0.11^{a}	2.19 ± 0.10^{a}	2.22 ± 0.07^{a}
	9.00%	2.11 ± 0.03^{b}	2.13 ± 0.05^{b}	2.29 ± 0.07^{a}
	12.00%	2.00 ± 0.01^{b}	2.06 ± 0.04^{b}	2.21 ± 0.05^{a}
	15.00%	1.86 ± 0.05^{b}	1.97 ± 0.07^{b}	2.12 ± 0.07^{a}
FCR	3.00%	1.53 ± 0.16^{a}	1.61 ± 0.23^{a}	1.48 ± 0.03^{a}
	6.00%	1.47 ± 0.18^{a}	1.32 ± 0.15^{a}	1.25 ± 0.04^{a}
	9.00%	1.47 ± 0.05^{a}	1.3 ± 0.01^{ab}	1.15 ± 0.09^{b}
	12.00%	2.05 ± 0.08^{a}	1.64 ± 0.07^{b}	1.27 ± 0.05^{c}
	15.00%	2.81 ± 0.15^{a}	1.88 ± 0.08^{b}	1.45 ± 0.11^{c}
HSI (%)	3.00%	1.80 ± 0.19^{a}	1.74 ± 0.08^{a}	1.74 ± 0.07^{a}
	6.00%	2.11 ± 0.14^{a}	2.04 ± 0.19^{a}	2.13 ± 0.10^{a}
	9.00%	2.42 ± 0.06^{a}	2.25 ± 0.08^{a}	2.24 ± 0.16^{a}
	12.00%	3.02 ± 0.09^{a}	2.58 ± 0.09^{b}	2.29 ± 0.09^{c}
	15.00%	3.48 ± 0.11^{a}	2.86 ± 0.14^{b}	2.52 ± 0.16^{c}

No overlap in the labeled letters indicates a significant difference ($P < 0.05$)

W_0 Initial body weight, W_t Final body weight, *WGR* Weight gain rate, *SGR* Specific growth rate, *FCR* Feed conversion ratio, and *HSI* Hepatosomatic index

Calculation formulas are as follows:

$\text{WGR}\ (\%) = 100 \times (W_t - W_0)/W_0$

$\text{SGR}\ (\%) = 100 \times (\ln W_t - \ln W_0)/t$ (t = duration of the feeding trial in days)

$\text{FCR} = F/(W_t - W_0)$ (F = total feed intake)

$\text{HSI}\ (\%) = 100 \times W_h/W$ (W_h = individual liver weight; W = individual final body weight)

microbiotas in BTBT, with abundances similar to those in TC, play an important supporting role in the development of tolerance to a high-fat environment.

Liver transcriptomic remodeling supports mitochondrial and genetic stability in BTBT

The liver is the core organ of lipid metabolism in fish, and its gene expression remodeling is pivotal to the high-fat stress response (Tang et al. 2019). STEM analysis indicated that the module genes with elevated expression in the maternal parent BSB as lipid content increased were primarily involved in lipid metabolism (fatty acid transport) and immunosuppression processes (negative regulation of IL-6) (Fig. 5I). It optimized fat transport via lipid metabolism genes and may reduce high-fat inflammatory damage by inhibiting immune responses, which is consistent with the previous studies in zebrafish (Zhang et al. 2025a). In paternal TC, module genes that were upregulated with increasing lipid content were primarily concentrated in ER-related pathways (including protein folding and stress response) (Fig. 5J). High-fat-induced ER stress has also been

Table 3 Alpha diversity index of gut bacterial communities in BSB, TC, and BTBT

Sample	PD whole tree	Chao1	ACE	Shannon	Simpson	Observed species	Goods coverage
BSB_1	19.62^{cde}	191.39^{bcdef}	191.38^{bcdef}	3.89^{ef}	0.78^{def}	190.72^{bcdef}	1.00
BSB_2	21.70^{c}	181.72^{bcdf}	182.22^{bcdf}	3.26^{f}	0.73^{f}	181.12^{bcdf}	1.00
BSB_3	30.62^{a}	337.89^{a}	336.91^{a}	5.92^{a}	0.95^{abc}	336.70^{a}	1.00
BSB_4	21.34^{c}	192.43^{bc}	192.74^{bc}	3.70^{ef}	0.80^{ef}	191.72^{bc}	1.00
BSB_5	24.78^{b}	267.18^{a}	267.11^{a}	5.04^{cd}	0.90^{abcd}	266.47^{a}	1.00
TC_1	16.60^{e}	149.04^{e}	148.32^{e}	5.47^{abcd}	0.94^{abc}	148.38^{e}	1.00
TC_2	18.51^{cde}	173.16^{bcdef}	172.37^{bcdef}	5.23^{abcd}	0.90^{abcde}	172.55^{bcdef}	1.00
TC_3	15.56^{e}	144.30^{ef}	144.07^{e}	5.66^{abc}	0.97^{a}	143.75^{ef}	1.00
TC_4	16.24^{e}	145.45^{e}	145.30^{e}	5.71^{ab}	0.97^{ab}	144.62^{e}	1.00
TC_5	16.03^{e}	135.77^{e}	135.78^{e}	5.12^{cd}	0.95^{bc}	135.55^{e}	1.00
BTBT_1	17.48^{de}	161.66^{def}	162.01^{def}	5.10^{bcd}	0.92^{abc}	161.17^{def}	1.00
BTBT_2	22.03^{bc}	214.55^{b}	213.08^{b}	5.28^{abcde}	0.86^{abcdef}	213.40^{b}	1.00
BTBT_3	16.10^{e}	147.86^{ef}	147.26^{ef}	5.59^{abcd}	0.96^{ab}	147.43^{ef}	1.00
BTBT_4	17.75^{de}	154.76^{cdef}	154.57^{cdef}	4.61^{abcdef}	0.87^{abcde}	154.38^{cdef}	1.00
BTBT_5	21.38^{bcd}	203.61^{bcd}	203.51^{bcd}	4.97^{d}	0.92^{c}	202.45^{bcd}	1.00

No overlap in the labeled letters indicates a significant difference ($P < 0.05$)

BSB blunt snout bream; *TC* topmouth culter; *BTBT* hybrid culter derived from lineage of BSB ♀ × TC ♂; *PD* phylogenetic diversity

previously observed in *Acanthopagrus schlegelii* (Shen et al. 2023). Lipid metabolism disorders disrupt ER homeostasis, leading to the accumulation of unfolded/misfolded proteins; cells then activate ER stress pathways to restore their functions and physiological status (Chambers and Marciniak 2014). Accordingly, TC may alleviate high-fat-induced protein misfolding by activating the ER stress pathway. The BTBT module genes that were upregulated as the lipid content increased were enriched for mitochondrial function (such as respiratory chain assembly and electron transport) and genetic information processing (including mRNA splicing and rRNA metabolism) pathways (Fig. 5K). High expression of mitochondrial genes enhances lipid degradation and reduces liver lipid accumulation (Vamecq et al. 2012). This is consistent with the finding that pasteurized *Akkermansia muciniphila* improves lipid metabolism in zebrafish (Danio rerio) via mitochondrial function (Huang et al. 2024). In addition, upregulated genes involved in genetic information processing maintain gene expression accuracy under high-fat stress and reduce the risk of metabolic disorders (Park et al. 2021). BTBT alleviates high-fat stress by enhancing mitochondrial function and genetic information processing.

Multi-omics integration reveals coordinated host–microbe regulation in BTBT

Fish HFD adaptability is co-driven by a multilevel molecular regulatory network and the host's intestinal microbiome (Cao et al. 2025; Wu et al. 2024). GSEA indicated that BTBT exhibited expression advantages over BSB in HFD lipid metabolism pathways, such as PPAR signaling and fatty acid degradation (Fig. 6A). PPAR pathway regulation is central to maintaining lipid homeostasis (Bougarne et al. 2018), which suggests that BTBT maintains lipid balance via this pathway under HFD conditions. WGCNA revealed three DEG expression patterns in three species under HFD: BTBT with the lowest expression (grey60 module), BTBT with the highest expression (magenta module), and BTBT with intermediate expression (green, cyan, midnight blue, and brown modules) (Fig. 7C). Functional enrichment revealed that the grey60 module genes (lowest in BTBT) are involved in inflammatory regulation, such as positive T-cell migration. This indicates that BTBT exhibits lower HFD-induced inflammation, which matches the inflammatory factor expression levels of BTBT and its parents (Fig. 8A). Meanwhile, BTBT had significantly higher *Rhodobacter* abundance than its parental lines under HFD conditions (Fig. 8B). This genus has been confirmed to enhance the antioxidant capacity of fish (Liao et al. 2022). Pearson correlation analysis suggested that *Rhodobacter* was negatively correlated with most proinflammatory pathway genes in the grey60 module, with a significant negative correlation with *ela2l* ($P < 0.05$, Fig. 8C). High *ela2l* expression is often linked to fish inflammation (Liao et al. 2022); consequently, BTBT may inhibit liver inflammation and ensure high survival by enriching *Rhodobacter*, which is similar to how *Lactococcus lactis* fermentation products alleviate zebrafish HFD damage (Li et al. 2023). Furthermore, genes in the intermediate expression modules were significantly enriched in pathways related to five aspects: lipid metabolism, energy metabolism, antioxidant defense, immunity, and tissue repair (Fig. 7E, H, Supplementary Table S3). The core

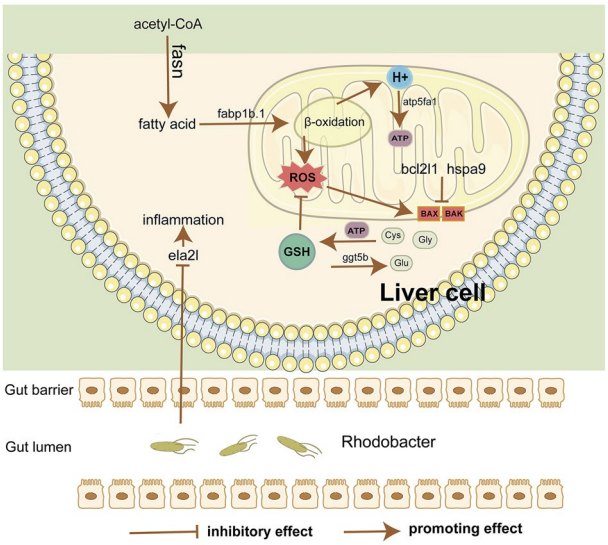

Fig. 9 Mechanism of hybrid culter derived from lineage of BSB ♀×TC ♂ (BTBT) in response to high-fat diet (HFD) conditions

genes in each pathway were screened out by constructing a PPI network using STRING and combining it with betweenness centrality analysis (Fig. 8D–H). Among these, *fasn* can regulate endogenous lipid synthesis (Hodson and Gunn 2019); *fabp1b.1* enhances fatty acid transport efficiency, promotes fatty acid entry into mitochondria for β-oxidation, and thereby maintains liver lipid homeostasis (Zhang et al. 2024); *atp5fa1* is involved in ATP synthesis in mitochondria and provides energy for GSH synthesis, which can scavenge reactive oxygen species (Xian et al. 2025); *ggt5b* participates in GSH degradation and coordinates intracellular GSH homeostasis by regulating its degradation rate (Timme-Laragy et al. 2013); *bcl2l1* and *hspa9* bind to pro-apoptotic Bcl-2-associated X and Bcl-2 homologous antagonist/killer proteins, thereby preventing their conformational changes and oligomerization and inhibiting their pro-apoptotic activity at the source (Sarfaraz et al. 2020; Valleh et al. 2014). The expression patterns of these key genes in BTBT demonstrate the integrative characteristics of its parents, forming a more comprehensive regulatory network that confers BTBT greater HFD adaptability (Fig. 9).

Conclusions

In conclusion, this study elucidates the HFD adaptation mechanism of BTBT, integrating the advantages of its parental lines, including growth performance, liver histology, nutrient absorption capacity, gut microbiota stability, comprehensive regulation of multi-pathway genes, and anti-inflammatory effects of signature genera. BTBT exhibits superior growth tolerance under HFD conditions and robust liver health. BTBT possesses moderate lipid digestion capacity; it optimizes lipid metabolism and inhibits inflammation by stabilizing the gut microbiota. Moreover, it maintains molecular homeostasis under HFD conditions by enhancing mitochondrial function and genetic information processing and integrates key parental genes to establish a multi-dimensional regulatory network. This cross-level coordinated regulation underpins its high survival rate and high-fat adaptability while providing theoretical and germplasm support for improving stress-resistant germplasm in aquaculture.

Supplementary Information The online version contains supplementary material available at https://doi.org/10.1007/s42995-026-00389-y.

Acknowledgements This research was financially supported by grants from the Yuelushan Laboratory Breeding Program (Grant No. YLS-2025-ZY01011); the National Natural Science Foundation of China (Grant Nos. 32102781, 32293250, and 32293251); the Key Research and Development Program of Hunan Province (Grant No. 2023WK2001); the Natural Science Foundation of Hunan Province, China (Grant Nos. 2024JJ6314 and 2023JJ40075); and the Changsha Municipal Natural Science Foundation (Grant No. kq2402160).

Author contributions YW designed the study and wrote the manuscript. CX JH and XH performed the experiments. JZ and XH provided the experimental methods. WM and ZW provided analysis software. HL and FH performed the data analysis. LQ and JH participated in the figure creation. CW and SL reviewed and edited the manuscript. All authors have read and agreed to the published version of the manuscript.

Data availability The complete clean reads for the libraries used in this study have been uploaded to the NCBI Sequence Read Archive (SRA) site (http://www.ncbi.nlm.nih.gov/sra/; BioProject ID: PRJNA1367943 and PRJNA1367878).

Declarations

Conflict of interest The authors declare that they have no competing interests.

Animal and human rights statement This research was reviewed and approved by the Animal Care and Welfare Committee of the Biomedical Research Ethics Committee at Hunan Normal University (Changsha, Hunan, China) (Approval Number: 2023 No. (610)). In addition, all fish were humanely anesthetized with 100 mg/L MS-222 before dissection.

Open Access This article is licensed under a Creative Commons Attribution-NonCommercial-NoDerivatives 4.0 International License, which permits any non-commercial use, sharing, distribution and reproduction in any medium or format, as long as you give appropriate credit to the original author(s) and the source, provide a link to the Creative Commons licence, and indicate if you modified the licensed material. You do not have permission under this licence to share adapted material derived from this article or parts of it. The images or other third party material in this article are included in the article's Creative Commons licence, unless indicated otherwise in a credit line to the material. If material is not included in the article's Creative Commons licence and your intended use is not permitted by statutory regulation or exceeds

the permitted use, you will need to obtain permission directly from the copyright holder. To view a copy of this licence, visit http://creativecommons.org/licenses/by-nc-nd/4.0/.

References

Adjoumani JY, Wang K, Zhou M, Liu W, Zhang D (2017) Effect of dietary betaine on growth performance, antioxidant capacity and lipid metabolism in blunt snout bream fed a high-fat diet. Fish Physiol Biochem 43:1733–1745

Bonvini E, Parma L, Mandrioli L, Sirri R, Brachelente C, Mongile F, Gatta PP, Bonaldo A (2015) Feeding common sole (*Solea solea*) juveniles with increasing dietary lipid levels affects growth, feed utilization and gut health. Aquaculture 449:87–93

Bougarne N, Weyers B, Desmet SJ, Deckers J, Ray DW, Staels B, De Bosscher K (2018) Molecular actions of PPAR α in lipid metabolism and inflammation. Endocr Rev 39:760–802

Boujard T, Gélineau A, Covès D, Corraze G, Dutto G, Gasset E, Kaushik S (2004) Regulation of feed intake, growth, nutrient and energy utilisation in European sea bass (*Dicentrarchus labrax*) fed high fat diets. Aquaculture 231:529–545

Cao X, Huang Y, Chu X, Wang X, Zheng S, Shi X, Xiang X, Miao L, Liu W, Jiang G (2025) Differential pathways to hepatic steatosis in fish: divergent molecular mechanisms underlying high-carbohydrate versus high-lipid diet-induced lipid accumulation. Aquacult Rep 45:103090

Chambers J, Marciniak S (2014) Cellular mechanisms of endoplasmic reticulum stress signaling in health and disease. 2. Protein misfolding and ER stress. Am J Physiol Cell Physiol 307:C657–C670

Chang J, Niu H, Jia Y, Li S, Xu G (2018) Effects of dietary lipid levels on growth, feed utilization, digestive tract enzyme activity and lipid deposition of juvenile *Manchurian trout*, *Brachymystax lenok* (Pallas). Aquacult Nutr 24:694–701

Chen W, Gao S, Chang K, Zhao X, Niu B (2023a) Dietary sodium butyrate supplementation improves fish growth, intestinal microbiota composition, and liver health in largemouth bass (*Micropterus salmoides*) fed high-fat diets. Aquaculture 564:739040

Chen Y, Xiong Z, Qin P, Liu Q, Fan Y, Xu Q, Wang X, Yang Z, Li W, Wen M (2023b) A comparative study of muscle nutrition and intermuscular bone number in improved diploid carp. Reprod Breed 3:118–124

Chi Y, Bai Z, Feng G, Lai X, Song Y (2024) ER–mitochondria contact sites regulate hepatic lipogenesis via Ip3r-Grp75-Vdac complex recruiting Seipin. Cell Commun Signal 22:464

Desouky H, Sayed N, Abasubong K, Zhang Z (2025) Nutritional and physiological effects of high-fat diets in finfish: effects on growth, immunity, lipid metabolism, and intestinal health: a review. J Comp Physiol B 195:415–437

Dessen J, Østbye T, Ruyter B, Bou M, Thomassen M, Rørvik K (2021) Sudden increased mortality in large seemingly healthy farmed Atlantic salmon (*Salmo salar* L.) was associated with environmental and dietary changes. J Appl Aquacult 33:165–182

Estensoro I, Ballester-Lozano G, Benedito-Palos L, Grammes F, Martos-Sitcha JA, Mydland L-T, Calduch-Giner JA, Fuentes J, Karalazos V, Ortiz A (2016) Dietary butyrate helps to restore the intestinal status of a marine teleost (*Sparus aurata*) fed extreme diets low in fish meal and fish oil. PLoS ONE 11:e0166564

Greene D, Selivonchick D (1987) Lipid metabolism in fish. Prog Lipid Res 26:53–85

Guo J, Zhou Y, Zhao H, Chen W, Chen Y, Lin S (2019) Effect of dietary lipid level on growth, lipid metabolism and oxidative status of largemouth bass, *Micropterus salmoides*. Aquaculture 506:394–400

Han C, Wen X, Zheng Q, Li H (2011) Effects of dietary lipid levels on lipid deposition and activities of lipid metabolic enzymes in hybrid tilapia (*Oreochromis niloticus*× *O. aureus*). J Anim Physiol Anim Nutr 95:609–615

He L, Zhang Y, Cao Q, Shan H, Zong J, Feng L, Jiang W, Wu P, Zhao J, Liu H (2024) Hepatic oxidative stress and cell death influenced by dietary lipid levels in a fresh teleost. Antioxidants (Basel) 13:808

Hodson L, Gunn PJ (2019) The regulation of hepatic fatty acid synthesis and partitioning: the effect of nutritional state. Nat Rev Endocrinol 15:689–700

Hooper L, Littman D, Macpherson A (2012) Interactions between the microbiota and the immune system. Science 336:1268–1273

Huang Z, Wang Y, Feng S, Zhang Y, Zhang X, Chang X, Yang G, Meng X (2024) Effects of pasteurized *Akkermansia muciniphila* on lipid metabolism disorders induced by high-fat diet in zebrafish (*Danio rerio*). Aquacult Rep 38:102363

Huang H, Tian X, Chen H, He Y, Chen Y, Lin S (2025) Transcriptomic analysis reveals sexual dimorphism in lipid metabolism within largemouth bass (*Micropterus salmoides*) fed the high-fat diet. Comp Biochem Physiol D 55:101533

Jandhyala S, Talukdar R, Subramanyam C, Vuyyuru H, Sasikala M, Reddy D (2015) Role of the normal gut microbiota. World J Gastroenterol 21:8787

Jia R, Hou Y, Zhou L, Zhang L, Li B, Zhu J (2024) Comparative transcriptome analysis reveals the impact of a high-fat diet on hepatic metabolic function in tilapia (*Oreochromis niloticus*). Animals 14:3204

Jiang X, Song Z, Li C, Hu X, Ge Y, Cheng L, Shi X, Jia Z (2024) Effects of dietary lipid levels on the growth, muscle fatty acid and amino acid composition, antioxidant capacity, and lipid deposition in mirror carp (*Cyprinus carpio*). Animals 14:2583

Jiao F, Zhang L, Limbu SM, Yin H, Xie Y, Yang Z, Shang Z, Kong L, Rong H (2023) A comparison of digestive strategies for fishes with different feeding habits: digestive enzyme activities, intestinal morphology, and gut microbiota. Ecol Evol 13:e10499

Jin M, Pan T, Tocher D, Betancor M, Monroig Ó, Shen Y, Zhu T, Sun P, Jiao L, Zhou Q (2019) Dietary choline supplementation attenuated high-fat diet-induced inflammation through regulation of lipid metabolism and suppression of NFκB activation in juvenile black seabream (*Acanthopagrus schlegelii*). J Nutr Sci 8:e38

Khadim S, Fatima M, Shah S, Azmat H, Rashid M (2025) Protein sparing by dietary lipids in the diets of *Pangasianodon hypophthalmus*: an appraisal of growth, body composition, digestive enzymes, and metabolic responses. Fish Physiol Biochem 51:134

Langfelder P, Horvath S (2008) WGCNA: an R package for weighted correlation network analysis. BMC Bioinform 9:559

Li X, Liu W, Jiang Y, Zhu H, Ge X (2010) Effects of dietary protein and lipid levels in practical diets on growth performance and body composition of blunt snout bream (*Megalobrama amblycephala*) fingerlings. Aquaculture 303:65–70

Li S, Yang H, Jin Y, Hao Q, Liu S, Ding Q, Yao Y, Yang Y, Ran C, Wu C (2023) Dietary cultured supernatant mixture of *Cetobacterium somerae* and *Lactococcus lactis* improved liver and gut health, and gut microbiota homeostasis of zebrafish fed with high-fat diet. Fish Shellfish Immunol 142:109139

Li C, Wang W, Wen X, Qi S, Xu J, Wu D, Tian K, Zhang C, Zhang B, Ma Q (2025) The microbiome, metabolome, and correlation analysis reveal the beneficial role of the commensal *Shewanella* sp. MR-7 in foodborne enteritis in turbot (*Scophthalmus maximus* L.). Aquaculture 603:742387

Liang X, Chen P, Wu X, Xing S, Morais S, He M, Gu X, Xue M (2022) Effects of high starch and supplementation of an olive extract on the growth performance, hepatic antioxidant capacity and lipid

metabolism of largemouth bass (*Micropterus salmoides*). Antioxidants 11:577

Liao Z, Gong Y, Zhao W, He X, Wei D, Niu J (2022) Comparison effect of *Rhodobacter sphaeroides* protein replace fishmeal on growth performance, intestinal morphology, hepatic antioxidant capacity and immune gene expression of *Litopenaeus vannamei* under low salt stress. Aquaculture 547:737488

Liu C, Zhao L, Shen Y (2021a) A systematic review of advances in intestinal microflora of fish. Fish Physiol Biochem 47:2041–2053

Liu P, Wang Y, Yang G, Zhang Q, Meng L, Xin Y, Jiang X (2021b) The role of short-chain fatty acids in intestinal barrier function, inflammation, oxidative stress, and colonic carcinogenesis. Pharmacol Res 165:105420

Lu K, Xu W, Li J, Li X, Huang G, Liu W (2013) Alterations of liver histology and blood biochemistry in blunt snout bream *Megalobrama amblycephala* fed high-fat diets. Fish Sci 79:661–671

Luo K, Deng Y, Han L, Wang S, Zhang Y, Pen Z, Liu T, Wang C, Liu C, Tao M (2024) Comparative study of hypoxic tolerance between the hybrids of white crucian carp (♀)× red crucian carp (♂) and its parents. Reprod Breed 4:164–173

Ma Q, Li L, Le J, Lu D, Qiao F, Zhang M, Du Z, Li D (2018) Dietary microencapsulated oil improves immune function and intestinal health in Nile tilapia fed with high-fat diet. Aquaculture 496:19–29

Ma J, Kong L, Zhou S, Lin H, Lin Y, Qin H, Long Z, Liu L, Huang Z, Li Z (2023) Effect of supplementation of chlorogenic acid to high-fat diet on growth, lipid metabolism, intestinal and hepatic histology, and gut microbiota of spotted sea bass (*Lateolabrax maculatus*). Metabolites 13:1067

Manoharan R, Han K, Shin H, Lee Y, Baek S, Moon E, Park Y, Cho J, Srinivasan S (2025) Modulation of gut microbiota and antibiotic resistance genes by heat-killed *Enterococcus faecalis* EF-2001 in high-fat diet-induced obesity mice: A shotgun metagenomics study. Bioengineering 12:741

Min Y, Rhee P (2015) The role of microbiota on the gut immunology. Clin Ther 37:968–975

Naiel M, Negm S, Ghazanfar S, Shukry M, Abdelnour S (2023) The risk assessment of high-fat diet in farmed fish and its mitigation approaches: a review. J Anim Physiol Anim Nutr 107:948–969

Park Y, Han S, Huh J, Kim J (2021) Emerging roles of epigenetic regulation in obesity and metabolic disease. J Biol Chem 297:101296

Sarfaraz S, Singh S, Hawke A, Clarke ST, Ramdath DD (2020) Effects of high-fat diet induced obesity and fructooligosaccharide supplementation on cardiac protein expression. Nutrients 12:3404

Sargent J, Bell G, McEvoy L, Tocher D, Estevez A (1999) Recent developments in the essential fatty acid nutrition of fish. Aquaculture 177:191–199

Sharma M, Pudlo N, Järvå MA, Kaur A, John A, Burchill L, Lingford JP, Epa R, Abayakoon P, Scott NE (2025) Sulfoglycolysis sustains *Eubacterium rectale* in low-fiber diets. J Biol Chem 301:108320

Shen Y, Zhao W, Bao Y, Zhu J, Jiao L, Duan X, Pan T, Monroig Ó, Zhou Q, Jin M (2023) Molecular cloning and characterization of endoplasmic reticulum stress related genes grp78 and atf6α from black seabream (*Acanthopagrus schlegelii*) and their expressions in response to nutritional regulation. Fish Physiol Biochem 49:1115–1128

Snellman E, Colwell R (2004) *Acinetobacter* lipases: molecular biology, biochemical properties and biotechnological potential. J Ind Microbiol Biotechnol 31:391–400

Song F, Qin Y, Geng H, He C, Yang P, Wang W, Chen Y (2023) Transcriptome analysis reveals the effects of dietary lipid level on growth performance and immune response in golden pompano (*Trachinotus ovatus*). Aquaculture 563:738959

Sun H, Wang Y, Liu Y, Liu Y, Zhang J (2025) Dietary geniposide supplementation alleviates hepatic lipid deposition and oxidative stress induced by high-fat diet in juvenile tiger puffer, *Takifugu rubripes*. Aquac Rep 41:102711

Tang T, Hu Y, Peng M, Chu W, Hu Y, Zhong L (2019) Effects of high-fat diet on growth performance, lipid accumulation and lipid metabolism-related MicroRNA/gene expression in the liver of grass carp (*Ctenopharyngodon idella*). Comp Biochem Physiol B 234:34–40

Thapa S, Mishra J, Arora N, Mishra P, Li H, O′ Hair J, Bhatti S, Zhou S (2020) Microbial cellulolytic enzymes: diversity and biotechnology with reference to lignocellulosic biomass degradation. Rev Environ Sci Biotechnol 19:621–648

Thirunavukkarasar R, Kumar P, Sardar P, Sahu NP, Harikrishna V, Singha KP, Shamna N, Jacob J, Krishna G (2022) Protein-sparing effect of dietary lipid: changes in growth, nutrient utilization, digestion and IGF-I and IGFBP-I expression of Genetically Improved Farmed Tilapia (GIFT), reared in inland ground saline water. Anim Feed Sci Technol 284:115150

Timme-Laragy A, Goldstone J, Imhoff B, Stegeman J, Hahn M, Hansen J (2013) Glutathione redox dynamics and expression of glutathione-related genes in the developing embryo. Free Radic Biol Med 65:89–101

Valleh M, Hyttel P, Rasmussen M, Strøbech L (2014) Insulin-like growth factor 2: a modulator of anti-apoptosis related genes (HSP70, BCL2-L1) in bovine preimplantation embryos. Theriogenology 82:942–950

Vamecq J, Dessein A, Fontaine M, Briand G, Porchet N, Latruffe N, Andreolotti P, Cherkaoui-Malki M (2012) Mitochondrial dysfunction and lipid homeostasis. Curr Drug Metab 13:1388–1400

Wang Y, Luo Y, Geng C, Liao A, Zhao R, Tan H, Yao J, Wang S, Luo K, Qin Q (2022) Production of a diploid hybrid with fast growth performance derived from the distant hybridization of *Hypophthalmichthys nobilis* (female)× *Megalobrama amblycephala* (male). Reprod Breed 2:56–64

Wei F, Jiang H, Zhu C, Zhong L, Lin Z, Wu Y, Song L (2024a) The co-fermentation of whole-grain black barley and quinoa improves murine cognitive impairment induced by a high-fat diet via altering gut microbial ecology and suppressing neuroinflammation. Food Funct 15:11667–11685

Wei M, Song L, Yuan X, Li H, Ji H, Sun J (2024b) Dietary supplementation with a PPARγ agonist promotes adipocyte hyperplasia and improves high-fat diet tolerance and utilization in grass carp (*Ctenopharyngodon idellus*). Aquaculture 578:740081

Wu C, Huang X, Chen Q, Hu F, Zhou L, Gong K, Fu W, Gong D, Zhao R, Zhang C (2020) The formation of a new type of hybrid culter derived from a hybrid lineage of *Megalobrama amblycephala* (♀)× *Culter alburnus* (♂). Aquaculture 525:735328

Wu S, Pan M, Zan Z, Jakovlić I, Zhao W, Zou H, Ringø E, Wang G (2024) Regulation of lipid metabolism by gut microbiota in aquatic animals. Rev Aquacult 16:34–46

Xian C, Luo Q, Li W, Zou L, Liu J (2025) ATP5F1A deficiency causes developmental delay and motor dysfunction in humans and zebrafish. J Transl Med 23:1054

Xun P, Zhuang S, Yao H, Su J, Yang Y, Shu H, Yu W, Lin H (2024) Effects of sodium acetate supplementation on growth, hematologic and plasma biochemical parameter, lipid deposition, and intestinal health of juvenile golden pompano *Trachinotus ovatus* fed high-lipid diets. Aquacult Nutr 2024:7904141

Yin P, Xie S, Zhuang Z, He X, Tang X, Tian L, Liu Y, Niu J (2021) Dietary supplementation of bile acid attenuate adverse effects of high-fat diet on growth performance, antioxidant ability, lipid accumulation and intestinal health in juvenile largemouth bass (*Micropterus salmoides*). Aquaculture 531:735864

Zhang M, Yang X (2016) Effects of a high fat diet on intestinal microbiota and gastrointestinal diseases. World J Gastroentero 22:8905

Zhang Y, Song L, Liu R, Zhao Z, He H, Fan Q, Shen Z (2016) Effects of dietary protein and lipid levels on growth, body composition and flesh quality of juvenile topmouth culter, *Culter alburnus Basilewsky*. Aquacult Res 47:2633–2641

Zhang Y, Jiang Z, Han S, Li L, Qiao F, Zhang M, Du Z (2020) Inhibition of intestinal lipases alleviates the adverse effects caused by high-fat diet in Nile tilapia. Fish Physiol Biochem 46:111–123

Zhang Y, Fan H, Gao K, Zhang S, Lu R, Cao X, Xu X, Liu J (2024) Identification, tissue expression, and response to various fatty acid inductions of the fabp gene family in grass carp (*Ctenopharyngodon idella*). Aquacult Rep 39:102386

Zhang F, Tian J, Li J, Zhang T, Wang X (2025a) ILA mitigates HFD-induced metabolic dysfunction via lipid-immune crosstalk and gut microbiota modulation in zebrafish. Fish Shellfish Immunol 167:110683

Zhang L, Liao K, Shi P, Xie F, Xu J (2025b) Dietary microalgal mixture improve survival, growth performance, lipid metabolism, and inflammation in black seabream (*Acanthopagrus schlegelii*) fed high-fat diet. Aquaculture 607:742647

Zhang X, Liu F, Li B, Duan L, Yu J, Huang Z, Huang S, Liu H, Liu Q, Liu S (2025c) Multi-omics reveals the molecular mechanisms of rapid growth in distant hybrid fish. Aquaculture 596:741783

Zhou Q, Pu Y, Deng H, Gong J, Guo L, Ma J, Liu L, Yuan S, Chen Y, Su Y (2025) *Rhodobacter sphaeroides* reduces Pb accumulation by reshaping the intestinal microenvironment and improving liver oxidant resistance in common carp (*Cyprinus carpio* L.). J Hazard Mater 492:138152

Publisher's Note Springer Nature remains neutral with regard to jurisdictional claims in published maps and institutional affiliations.